Langmuir
Article
pubs.acs.org/Langmuir

Surface Potentials in Langmuir Monolayers of Unidirectionally Oriented α-Helical Diblock Copolypeptides

Le-Thu T. Nguyen, Aditya Ardana, Gerrit ten Brinke, and Arend J. Schouten*

Department of Polymer Chemistry, Zernike Institute for Advanced Materials, University of Groningen, Nijenborgh 4, 9747 AG Groningen, The Netherlands

Received October 21, 2009. Revised Manuscript Received December 3, 2009

The surface potentials and effective dipole moments of α-helical amphiphilic diblock copolypeptides during monolayer compression at the air−water interface are reported. Amphiphilic diblock copolypeptides (PLGA-*b*-PMLGSLGs) of poly(α-L-glutamic acid) (PLGA) and poly(γ-methyl-L-glutamate-*ran*-γ-stearyl-L-glutamate) with 30 mol % of stearyl substituents (PMLGSLG) of various block lengths were studied during the double-brush formation process at the water surface. Upon monolayer spreading of PLGA-*b*-PMLGSLGs, surface potentials of hundreds of millivolts were recorded, attributed to the dipole moments of water molecules reorienting due to interactions with the monolayers. Upon compression, the effective dipole moments derived from the surface potentials of the PLGA-*b*-PMLGSLG monolayers decrease gradually, most likely as a result of the immersion of the hydrophilic block in water and cancellation of the interactions between the hydrophobic block and the underlying water molecules. The polypeptide macrodipole moment immersed in water was apparently effectively screened out. The remaining effective dipole moment of the monolayer contributes mainly to the hydrophobic block, and upon tilting away from the water surface toward the surface normal, it was found to increase with the hydrophobic block length, indicating the gradual formation of unidirectional aligned polypeptide molecules in the double-brush monolayer.

Introduction

There has been a considerable interest in the fabrication of ultrathin films of unidirectionally oriented α-helical polypeptides because of their intriguing electro-optical properties arising from the large degree of polar order they exhibit.[1−9] Approaches to orient the α-helical chains of polypeptides at interfaces include application of an electric field[10] as well as the surface-grafting[11−17] and Langmuir−Blodgett techniques.[18−24] The large net dipole built up by the additive helix macrodipoles of vertically aligned parallel helices in surface-grafted polyglutamate films has been indirectly assessed by measuring the electromechanical properties of the films.[25] Miura et al.[26] and Kimura et al.[27] evaluated the dipole moment via the measurement of surface potentials in self-assembled monolayers (SAMs) of α-helical peptide molecules, unidirectionally oriented on solid substrates using the Kelvin probe method. They showed that the absolute value of surface potential (in vacuum) was larger for the longer helix peptide and was influenced by the dipole of the functional group linkages between the peptide and the substrate. They also found that the surface potential of oriented α-helical peptide SAMs decreased with increasing temperature due to thermally induced structural perturbations.

However, until now demonstration of the effective dipoles and an understanding of the influence of the monolayer helix length vertically aligned at the air−water interface remain elusive. Although the helix dipole moment in vacuum is proportional to the number of peptide bonds in the helix,[1,28] its magnitude can be drastically influenced by the surrounding environment. For a protein in solution, the effects of solvent screening, resulting from the counter-orienting dipole moments of the water molecules in response to the charge distribution of the peptides, give rise to effectively lower peptide dipoles.[29] It has been implied that the dipole interactions of the helix termini in membrane proteins,

*Corresponding author. E-mail: A.J.Schouten@rug.nl.

(1) Hol, W. G. J.; van Duijnen, P. T.; Berendsen, H. J. C. *Nature* **1978**, *273*, 443.
(2) Morita, T.; Kimura, S.; Kobayashi, S.; Imanishi, Y. *J. Am. Chem. Soc.* **2000**, *122*, 2850.
(3) Whitesell, J. K.; Chang, H. K.; Fox, M. A.; Galoppini, E.; Watkins, D. M.; Fox, H.; Hong, B. *Pure Appl. Chem.* **1996**, *68*, 1469.
(4) Jones, G.; Vullev, V.; Braswell, E. H.; Zhu, D. *J. Am. Chem. Soc.* **2000**, *122*, 388.
(5) Machida, S.; Urano, T. I.; Sano, K.; Kawata, Y.; Sunohara, K.; Sasaki, H.; Yoshiki, M.; Mori, Y. *Langmuir* **1995**, *11*, 4838.
(6) Machida, S.; Urano, T. I.; Sano, K.; Kato, T. *Langmuir* **1997**, *13*, 576.
(7) Müller, M.; Kessler, B.; Lunkwitz, K. *J. Phys. Chem. B* **2003**, *107*, 8189.
(8) Balavoine, F.; Schultz, P.; Richard, C.; Mallouh, V.; Ebbesen, T. W.; Mioskowski, C. *Angew. Chem., Int. Ed.* **1999**, *38*, 1912.
(9) Galoppini, E.; Fox, M. A. *J. Am. Chem. Soc.* **1996**, *118*, 2299.
(10) Block, H.; Shaw, C. P. *Polymer* **1992**, *33*, 2459.
(11) Enriquez, E. P.; Samulski, E. T. *Mater. Res. Soc. Symp. Proc.* **1992**, *255*, 423.
(12) Chang, Y. C.; Frank, C. W. *Langmuir* **1998**, *14*, 326.
(13) Wieringa, R. H.; Siesling, E. A.; Werkman, P. J.; Angerman, H. J.; Vorenkamp, E. J.; Schouten, A. J. *Langmuir* **2001**, *17*, 6485.
(14) Luijten, J.; Groeneveld, D. Y.; Nijboer, G. W.; Vorenkamp, E. J.; Schouten, A. J. *Langmuir* **2007**, *23*, 8163.
(15) Wang, Y.; Chang, Y. C. *J. Am. Chem. Soc.* **2003**, *125*, 6376.
(16) Niwa, M.; Morikawa, M.; Higashi, N. *Angew. Chem., Int. Ed.* **2000**, *39*, 960.
(17) Wain, A. J.; Do, H. N. L.; Mandal, H. S.; Kraatz, H.-B.; Zhou, F. *J. Phys. Chem. C* **2008**, *112*, 14519.
(18) Toyotama, A.; Kugimiya, S.; Yonese, M.; Kinoshita, T.; Tsujita, Y. *Chem. Lett.* **1997**, *26*, 443.
(19) Hosokawa, H.; Kinoshita, T.; Tsujita, Y.; Yoshimizu, H. *Chem. Lett.* **1997**, *26*, 745.
(20) Kishihara, K.; Kinoshita, T.; Mori, T.; Okahata, Y. *Chem. Lett.* **1998**, *27*, 951.
(21) Doi, T.; Kinoshita, T.; Tsujita, Y.; Yoshimizu, H. *Bull. Chem. Soc. Jpn.* **2001**, *74*, 421.
(22) Yokoi, H.; Kinoshita, T. *Chem. Lett.* **2004**, *33*, 426.
(23) Niwa, M.; Takada, T.; Higashi, N. *J. Mater. Chem.* **1998**, *8*, 633.
(24) Higashi, N.; Koga, T.; Niwa, M. *Langmuir* **2000**, *16*, 3482.
(25) Jaworek, T.; Neher, D.; Wegner, G.; Wieringa, R. H.; Schouten, A. J. *Science* **1998**, *279*, 57.
(26) Miura, Y.; Kimura, S.; Kobayashi, S.; Iwamoto, M.; Imanishi, Y.; Umemura, J. *Chem. Phys. Lett.* **1999**, *315*, 1.
(27) Kimura, S.; Miura, Y.; Morita, T.; Kobayashi, S.; Imanishi, Y. *J. Polym. Sci., Part A: Polym. Chem.* **2000**, *38*, 4826.
(28) Wada, A. *Adv. Biophys.* **1976**, *9*, 1.
(29) Gabdoulline, R. R.; Wade, R. C. *J. Phys. Chem.* **1996**, *100*, 3868.

Scheme 1. Chemical Structure of PLGA-*b*-PMLGSLG and Simple Schematic Representation of the Double-Brush Structure in the PLGA-*b*-PMLGSLG Monolayer at the Air−Water Interface

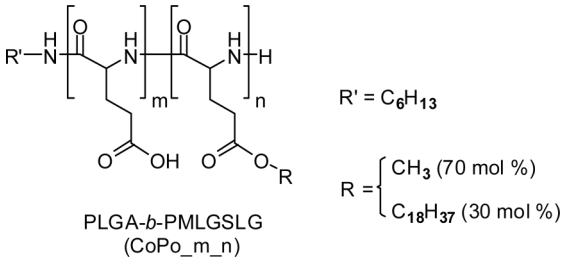

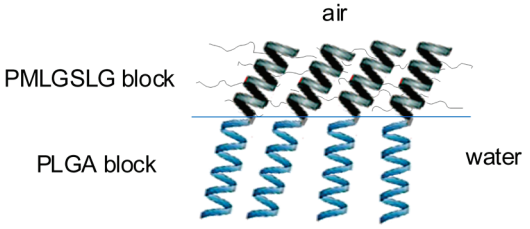

when close to the lipid−water interface, will be effectively screened by the solvent.[30,31] Sengupta et al.[32] calculated the effective helix dipole moment of the α-helical polyalanine of different lengths by simulation models in various environments corresponding to various positions of the helix relative to the aqueous medium. Though in aqueous solution the dipole moment of a polyalanine helix increased linearly with helix length, it was significantly smaller than the value obtained in vacuum. However, in a heterogeneous environment as found in a lipid membrane, polyalanine helices with the helix axis parallel to the membrane normal showed the opposite behavior such that the effective dipole moment decreased linearly with peptide length. This was attributed to the increased reaction field in the surrounding water induced by the approach of the terminal charges.

The present work concerns the assessment of the effective dipole of vertically oriented polypeptide helices at the air−water interface as a function of the peptide length. We have prepared α-helical poly(α-L-glutamic acid)-*b*-poly(γ-methyl-L-glutamate-*ran*-γ-stearyl-L-glutamate) with 30 mol % of stearyl substituents (PLGA-*b*-PMLGSLG) amphiphilic diblock copolymers of various block lengths. These diblock copolymers form a stable double brush with the α-helices unidirectionally aligned at the interfaces in Langmuir monolayers and Langmuir−Blodgett films (Scheme 1). The double-brush structure has been evidenced by surface pressure−area isotherms, Brewster angle microscopy, transmission FT-IR, and small-angle X-ray reflectivity measurements.[33] Here, the effective molecular dipole moments in the monolayers of the PLGA-*b*-PMLGSLG diblock copolymers of different block lengths at the air−water interface are evaluated by the study of surface potential using the Kelvin probe method.

Experimental Section

Materials. α-Helical PLGA-*b*-PMLGSLG was synthesized via a diblock copolymer precursor consisting of poly(γ-*tert*-butyl-L-glutamate) (PtBuLG) and PMLGSLG, with the *tert*-butyl group as a mild acid-labile, protecting group for the carboxylic acid.[33] PtBuLG-*b*-PMLGSLG was prepared by polymerization of tBuLG *N*-carboxyanhydrides (NCA) in chloroform at 0 °C using *n*-hexylamine initiator. PtBuLG was then used as macroinitiator for random copolymerization of γ-methyl and γ-stearyl L-glutamate (MLG and SLG) NCAs (70:30, mole ratio) in chloroform at 0 °C. The composition and purity of the diblock copolymers were confirmed by ^{1}H NMR ($CDCl_3$) and gel permeation chromatography (tetrahydrofuran eluent, polystyrene standard, universal calibration).[33,34] The degree of polymerization (DP) of PtBuLG was estimated from ^{1}H NMR ($CDCl_3$) using the integral ratio of the signal of the *tert*-butyl group ($(CH_3)_3$, 1.42 ppm) and that of the methyl group (CH_3, 0.87 ppm) of the *n*-hexylamine initiator incorporated in the polymer chain. The block length ratio of PtBuLG-*b*-PMLGSLG was determined by comparing the ^{1}H NMR peak integral of the *tert*-butyl group (9H, 1.42 ppm) with that of the stearyl group (30 H, 1.25 ppm). The *tert*-butyl group was removed using trifluoroacetic acid (TFA). PLGA-*b*-PMLGSLGs were notated as CoPo_*m*_*n*, where *m* and *n* the DPs of the PLGA and PMLGSLG blocks, respectively. PLGA (DP = 60) was obtained by hydrolysis of PtBuLG using TFA. PMLGSLG (DP = 89) was prepared by random copolymerization of MLG-NCA and SLG-NCA (70:30, mole ratio) in chloroform at 0 °C using triethylamine as initiator.

Surface Pressure−Area (π−A) Isotherms. π−A isotherms were measured using a home-modified computer-controlled Lauda Filmbalance (FW2), with an accuracy of 0.05 mN/m. The water used for the subphase was purified by reverse osmosis and subsequently through a Milli-Q filtration system. PLGA-*b*-PMLGSLGs were spread from *N*-methylpyrrolidone (NMP) (Acros, 99.5%)/chloroform (Lab-Scan, 99.5%), (3/7, v/v) solutions with 1−3% (v/v) of acetic acid (Acros, 99.5%) added, at a concentration of 0.4−0.6 mg/mL. PLGA was spread from a NMP/chloroform (3/7, v/v) solution at a concentration of 0.5 mg/mL. PMLGSLG was spread from a chloroform solution at a concentration of 0.6 mg/mL.

Surface Potential Measurements. Surface potential measurements were performed during compression of monolayers based on the noncontact vibrating plate technique using a commercial Kelvin probe KSV5000SPOT1 (KSV instruments, Helsinki, Finland). All experiments were carried out on pure water at 20 °C at a compression speed of ca. 16 cm^2 min^{-1}.

Results and Discussion

Surface potential−area (ΔV−A) isotherms, plotted together with the corresponding surface pressure−area (π−A) isotherms and the derived effective molecular dipole moment−area ($\mu_\perp$−A) curves, are given for PMLGSLG, PLGA, and PLGA-*b*-PMLGSLGs in Figures 1−3. Only ΔV starting from the onset of pressure buildup is presented. Prior to that, the potential was not uniform across the water surface due to the formation of aggregated monolayer islands inhomogeneously covering the water surface.[33] All the ΔV−A isotherms were measured on pure water. The surface potential can generally be expressed in terms of an effective molecular dipole moment ($\mu_\perp$), the component of the molecular dipole moment of the monolayer perpendicular to the water surface, using the Helmholtz equation:[35]

$$\frac{\mu_\perp}{\varepsilon} = \varepsilon_0 A \Delta V \qquad (1)$$

in which A is the molecular surface area; ε and ε_0 are the apparent relative permittivity of the monolayer and the permittivity of free space, respectively. $\mu_\perp$ can also be interpreted as the sum of contributions of different effective dipole moment components (capacitor model), μ_i, including the contribution of the underlying

(30) Gilson, M. K.; Honig, B. *Proc. Natl. Acad. Sci. U.S.A.* **1989**, *86*, 1524.
(31) Rogers, N. K.; Sternberg, M. J. E. *J. Mol. Biol.* **1984**, *174*, 527.
(32) Sengupta, D.; Behera, R. N.; Smith, J. C.; Ullmann, G. M. *Structure* **2005**, *13*, 849.
(33) Nguyen, L.-T. T.; Vorenkamp, E. J.; Daumont, C. J. M.; ten Brinke, G.; Schouten, A. J., submitted for publication.
(34) Temyanko, E.; Russo, P. S.; Ricks, H. *Macromolecules* **2001**, *34*, 582.
(35) Taylor, D. M. *Adv. Colloid Interface Sci.* **2000**, *87*, 183.

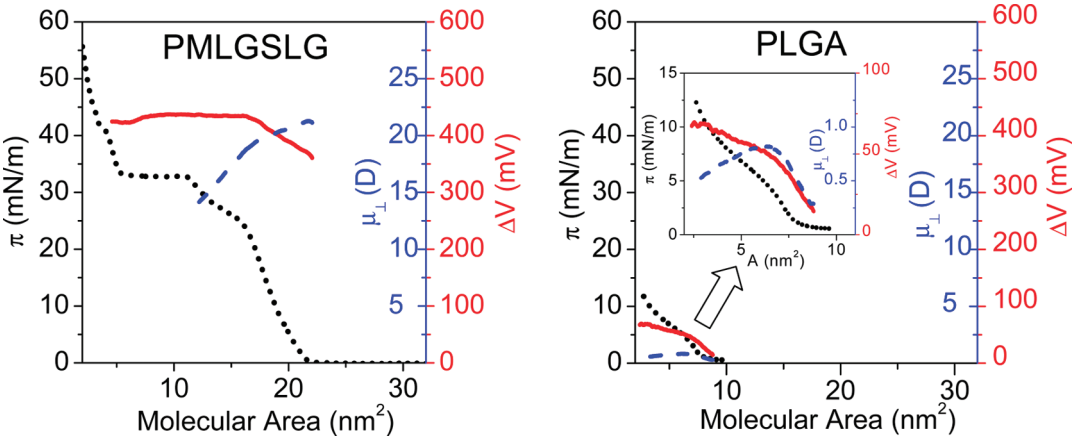

Figure 1. $\Delta V-A$ (solid red lines), $\mu_\perp-A$ (dashed blue lines), and $\pi-A$ (dotted black lines) isotherms on a pure water surface for monolayers of PMLGSLG (DP = 89) and PLGA (DP = 60). The $\mu_\perp-A$ plots were derived from the $\Delta V-A$ isotherms using the Helmholtz equation, assuming $\varepsilon = 1$.

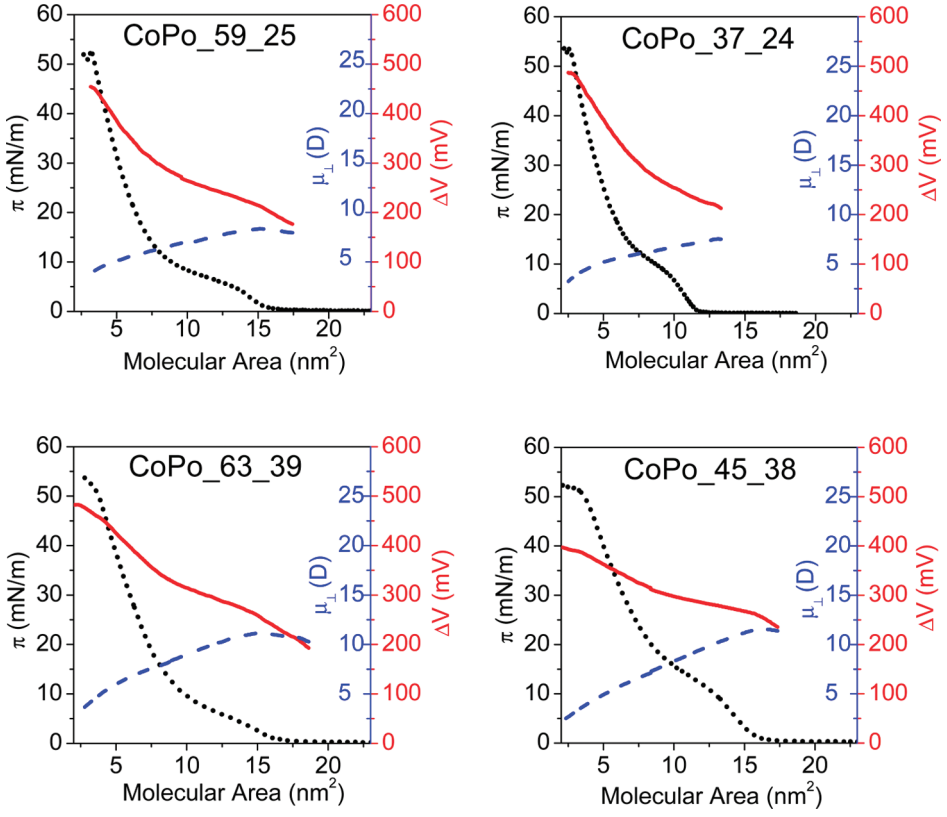

Figure 2. $\Delta V-A$ (solid red lines), $\mu_\perp-A$ (dashed blue lines), and $\pi-A$ (dotted black lines) isotherms on a pure water surface for monolayers of PLGA-*b*-PMLGSLG diblock copolymers of various PLGA block lengths. The $\mu_\perp-A$ plots were derived from the $\Delta V-A$ isotherms using the Helmholtz equation, assuming $\varepsilon = 1$.

water subphase,[36] as

$$\frac{\mu_\perp}{\varepsilon} = \sum \frac{\mu_i}{\varepsilon_i} \qquad (2)$$

where ε is the apparent relative permittivity of the monolayer and ε_i are the local relative permittivities.

Taking into account dipole−dipole interactions in the monolayer, ε strongly depends on the local fields of the polar groups and hence the orientation of the constituent dipoles in the monolayers as well as the density of the dipoles.[35] However, for a relative assessment and comparison of the effective dipoles in the monolayers studied, we simply derived $\mu_\perp$ from the measured ΔV by assuming that the monolayer is composed of a uniform assembly of molecular dipoles contributing equally to the polarization of the monolayer. In this case, the monolayer is considered to be analogous to a parallel-plate capacitor, and the relative permittivity of the air is assumed ($\varepsilon = 1$).[37]

As shown in Figure 1, the $\pi-A$ isotherm of PMLGSLG shows a steep rise in pressure upon compression due to the packing of the α-helices lying flat on the water surface, followed by a liquid-condensed phase and subsequently a plateau transition indicating

(36) Demchak, R. J.; Fort, T. J. *J. Colloid Interface Sci.* **1974**, *46*, 191.

(37) Taylor, D. M.; Bayes, G. F. *Phys. Rev. E* **1994**, *49*, 1439.

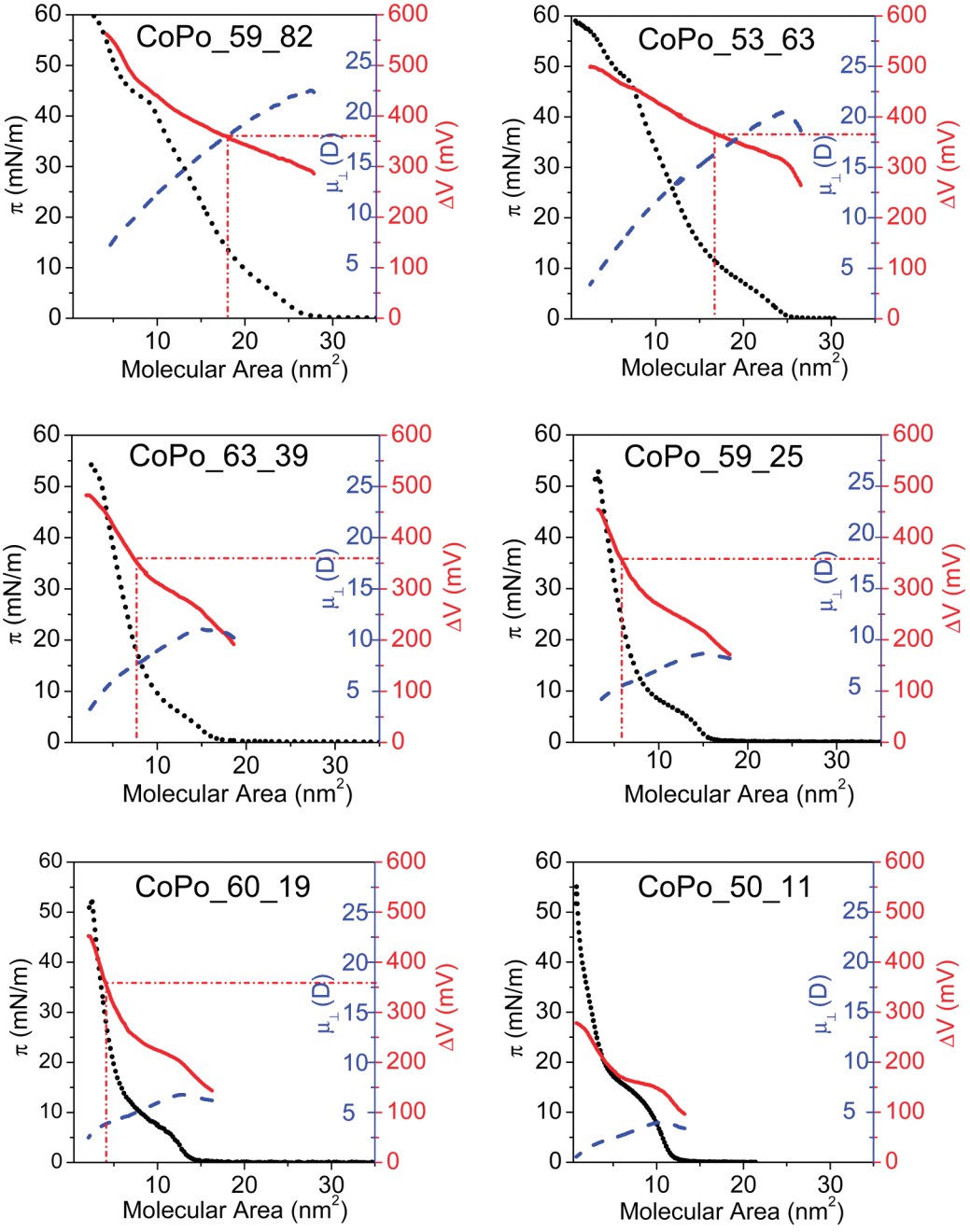

Figure 3. $\Delta V-A$ (solid red lines), $\mu_\perp-A$ (dashed blue lines), and $\pi-A$ (dotted black lines) isotherms on a pure water surface for monolayers of PLGA-*b*-PMLGSLG diblock copolymers of various PMLGSLG block lengths. The $\mu_\perp-A$ plots were derived from the $\Delta V-A$ isotherms using the Helmholtz equation, assuming $\varepsilon = 1$.

monolayer collapse.[38] The $\Delta V-A$ isotherm shows a curve form typical of homopolypeptides.[39,40] Hence, the explanation of the $\Delta V-A$ isotherm behavior previously reported by Malcolm[39−41] for polypeptides with side chain ester groups and those with hydrocarbon side chains can be applied to PMLGSLG. Therein the interactions of both the peptide and side chain polar groups with the underlying water accounting for a positive contribution to the potential were evident. Especially for polypeptides with ester groups in the side chains, the side chain length and conformation affect the side chain−water interactions and thereby the surface potential.[39] Because the helical rods are aligned parallel to the water surface, the peptide bond dipoles contribute inappreciably to $\mu_\perp$. $\mu_\perp$ is mainly due to polarization of the water molecules interacting with the polymer polar groups, wherein the positive end of the water molecular dipole is pointed upward. Besides, the local fields and orientations of the side chains may not be identical on the top and underneath the helices. Thus, the contribution to $\mu_\perp$ of the side chains may also be taken into account. As a result, a very high positive value of $\mu_\perp$ of 360 mV was recorded for PMLGSLG upon spreading. Upon monolayer compression, $\mu_\perp$ decreases slightly. Most likely this arises from side chain distortion since they tend to orient away from the water surface during molecular packing. In the liquid-condensed phase region, $\mu_\perp$ declines abruptly, indicative of a significant rotation of the side chain polar groups. In the plateau region corresponding

(38) Duda, G.; Schouten, A. J.; Arndt, T.; Lieser, G.; Schmidt, G. F.; Bubeck, C.; Wegner, G. *Thin Solid Films* **1988**, *159*, 221.
(39) Malcolm, B. R. *J. Polym. Sci., Part C* **1971**, *34*, 87.
(40) Malcolm, B. R. *Proc. R. Soc. London, Ser. A* **1968**, *305*, 363.
(41) Malcolm, B. R. *Polymer* **1966**, *7*, 595.

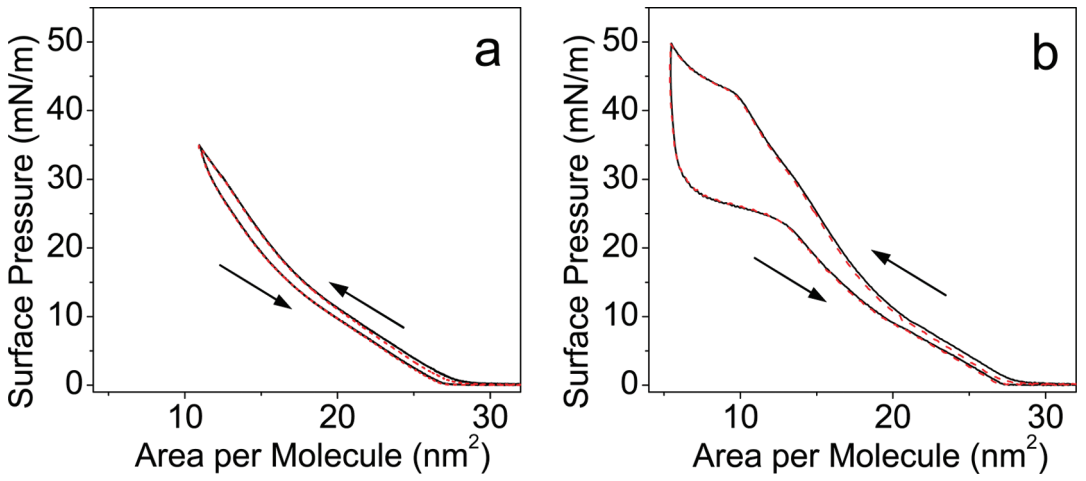

Figure 4. Compression−decompression $\pi-A$ isotherms of CoPo_59_82 at 20 °C on pure water surface with change from compression to decompression at 35 mN/m (a) and 50 mN/m (b). Solid black line: first cycle; dashed red line: second cycle. Susbsequent cycles are identical to the second one.

to monolayer collapse, interpretation of ΔV into $\mu_\perp$ using the Helmholtz relation is no longer appropriate.

PLGA is surface-active, showing a transition at a low surface pressure of ca. 5−7 mN/m in the $\pi-A$ isotherm (Figure 1). The monolayer exhibits very low values of ΔV and $\mu_\perp$. The $\mu_\perp$ for PLGA first increases slightly upon monolayer compression but then decreases when PLGA is fully immersed in water. It has been reported that the $\mu_\perp$ of polypeptides is largely suppressed in aqueous solution due to solvent screening effects.[32,42] Before the transition in the $\pi-A$ isotherm when the PLGA helices lie flat on the water surface, in contrast with the case of PMLGSLG, a very low $\mu_\perp$ of PLGA was recorded. This is probably because upon spreading, the COOH group of PLGA may form hydrogen bonds with the underlying water molecules via both the C═O (C═O···H−O) and OH (OC−OH···O−H) groups. While the first gives rise to orientation of water molecules with a positive water molecular dipole moment vertical to the surface, the latter results in a water molecular dipole moment in an opposite direction contributing negatively to $\mu_\perp$. Consequently, the dipole moment of the water molecules arising from interaction with the polymer is negligible.

The PLGA-*b*-PMLGSLG diblock copolymers display completely different $\pi-A$ and $\Delta V-A$ isotherms (Figures 2 and 3). Upon compression, the $\pi-A$ isotherms first show a transition at a low surface pressure which is attributed to the immersion of the PLGA block into the subphase.[33] The subsequent linear increment in surface pressure corresponds to compression and the tilting of the helices. All of the diblock copolymers show high collapse surface pressures of 50−55 mN/m. At high surface pressures, the molecular area lies in the range of the helix cross-sectional area of PMLGSLG, of 2.4−9.75 nm^2,[38] in agreement with a unidirectional alignment and a tilt of the helices. The second transition at a high surface pressure above 40 mN/m, only observed for CoPo_59_82 and CoPo_53_63, may be tentatively attributed to a transition from an isotropic phase (where the α-helices are oriented isotropically around the water surface normal with an average tilt angle with respect to the water surface) to a liquid-crystalline-like phase with a denser packing of the PMLGSLG segments.[43] As seen in Figure 4, the monolayer upon compression to a pressure above this transition shows a large hysteresis while before the transition the hysteresis is insignificant.

For all of the PLGA-*b*-PMLGSLGs, ΔV rises steadily during compression until the monolayer collapses. Because of the insignificant $\mu_\perp$ of the PLGA block, the initial positive value of $\mu_\perp$ for the PLGA-*b*-PMLGSLG monolayers upon spreading mainly arises from interactions between the PMLGSLG block lying on the water surface with the underlying water, as discussed above for PMLGSLG. Upon monolayer compression, $\mu_\perp$ first increases slightly but decreases as soon as the PLGA block is immersed in water. Because the α-helices are tilted from the water surface upon compression, the peptide dipole component vertical to the water surface is expected to increase. The decrease in the monolayer $\mu_\perp$ is probably caused by, in part, reorientations of the side chain polar components (ester and terminal methyl groups in the side chains) in a manner leading to a strong decrease in their vertical dipole moments. The changes in orientation and hence in the vertical dipole contribution during molecular packing of the polar components, such as the ester and terminal methyl groups in the side chains, are not readily distinguished. When the helices "stand up" at the interface, the hydrophobic helix layer composed of an array of unidirectionally oriented dipoles may give rise to a relative permittivity different from unity. This involves a number of factors including the dielectric anisotropy of constituent polar molecules as well as their orientational distribution, intermolecular interactions, and interactions of the dipoles with the water surface.[44] Furthermore, the local relative permittivities (ε_i) of the polar components may increase as the monolayer becomes more condensed.[35,37] More than likely, under tilting of the diblock copolymer molecules, the PMLGSLG hydrophobic block tends to leave the water surface. Consequently, the interactions between this block and the underlying water molecules, accounting for a considerably large initial $\mu_\perp$ contribution, are canceled out.

Because the peptide dipole moment of PLGA immersed in the water subphase is effectively screened, the contribution to $\mu_\perp$ of the PLGA block is negligible. As demonstrated in Figure 2, there are only small differences between the $\mu_\perp-A$ isotherms of PLGA-*b*-PMLGSLGs of various PLGA block lengths (DP_{PLGA}). However, varying the PMLGSLG block length ($DP_{PMLGSLG}$) leads to considerable changes of the values of ΔV and $\mu_\perp$. Comparison of

(42) Yamaoka, K.; Ichibakase, T.; Ueda, K.; Matsuda, K. *J. Am. Chem. Soc.* **1980**, *102*, 5109.
(43) Nguyen, L.-T. T.; Ardana, A.; Vorenkamp, E. J.; ten Brinke, G.; Schouten, A. J., manuscript in preparation.
(44) Wu, C.-X.; Iwamoto, M. *Phys. Rev. B* **1997**, *55*, 10922.

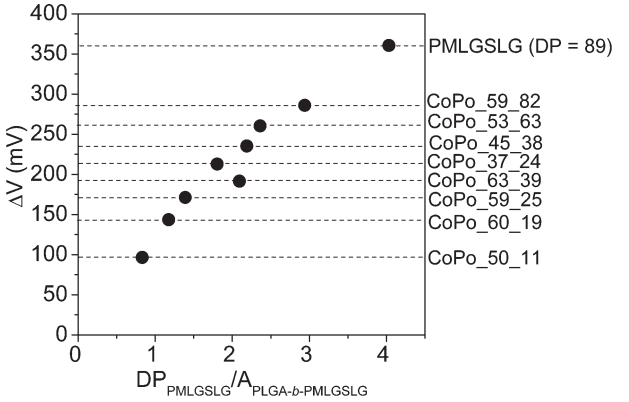

Figure 5. Surface potential at the onset surface pressure as a function of the surface area fraction of the PMLGSLG block.

Scheme 2. Simple Schematic Representation of the Arrangement of the PLGA-*b*-PMLGSLG Diblock Copolymers of Various Block Lengths at the Air−Water Interface at Onset Surface Pressures

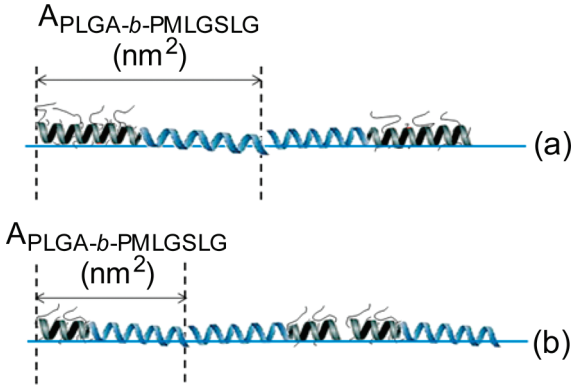

Scheme 3. Simple Schematic Representation of the Arrangement of the PLGA-*b*-PMLGSLG Diblock Copolymers at the Air−Water Interface after the Immersion of the PLGA Block in Water

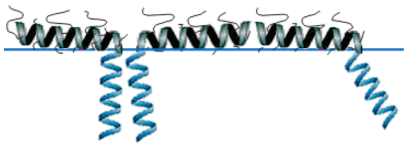

the isotherms for the monolayers of PLGA-*b*-PMLGSLGs with the different $DP_{PMLGSLG}$ is shown in Figure 3.

Upon spreading, since the initial high surface potential is produced mainly by the interaction of the PMLGSLG block with the water surface, ΔV is strongly related to the surface area occupied by the PMLGSLG block. At the onset of surface pressure buildup, the α-helical molecules of the PLGA-*b*-PMLGSLG diblock copolymers are lying flat on the water surface as described in Scheme 2. Thus, both $DP_{PMLGSLG}$ and DP_{PLGA} influence the initial value of ΔV. As seen in Figure 5, ΔV at the onset pressure increases linearly with $DP_{PMLGSLG}/A_{PLGA\text{-}b\text{-}PMLGSLG}$, where $A_{PLGA\text{-}b\text{-}PMLGSLG}$ is the molecular surface area of PLGA-*b*-PMLGSLG at the onset pressure. This clearly shows that the surface area fraction of the PMLGSLG block determines the initial value of surface potential upon monolayer spreading.

Assuming that the PMLGSLG hydrophobic block segments lie flat covering the entire water surface just before they start to tilt away from the surface as described in Scheme 3, the monolayer surface potential of PLGA-*b*-PMLGSLG should be about equal to that of PMLGSLG at the onset of surface pressure buildup,

Scheme 4. Simple Schematic Representation of the Arrangement of the PLGA-*b*-PMLGSLG Diblock Copolymers of Various Block Lengths at the Air−Water Interface at High Surface Pressures, Being Tilted Away from the Water Surface

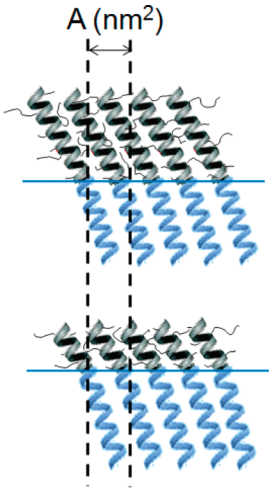

i.e., about 360 mV, irrespective of $DP_{PMLGSLG}$. The point in the $\pi-A$ isotherm where $\Delta V = 360$ mV is indicated in Figure 3 for the different PLGA-*b*-PMLGSLGs. For the diblock copolymers with a large $DP_{PMLGSLG}$, the point where $\Delta V = 360$ mV occurs immediately after the first transition corresponding to the water immersion of the PLGA block. However, when $DP_{PMLGSLG} < 40$, the point where $\Delta V = 360$ mV is shifted to a smaller surface area and higher surface pressure. Apparently for a small $DP_{PMLGSLG}$, the PMLGSLG block segments are already tilted soon after the first transition. With the very small $DP_{PMLGSLG}$ of CoPo_50_11, the PMLGSLG block acts like an anchor, so that the situation where the PMLGSLG block lies flat covering the entire water surface cannot be achieved.

At high surface pressures, corresponding to molecular surface areas ≤10 nm^2 (the maximum cross-sectional area of a PMLGSLG helix), the helices are tilted away from the water surface forming a double-brush structure (Scheme 4). Since the average helix tilt angle of the PMLGSLG block is determined by the surface chain density at the interface, at the same molecular surface area, the same average helix tilt angle of the PMLGSLG block is obtained for the PLGA-*b*-PMLGSLG diblock copolymers of various block lengths (Scheme 4). Figure 6 compares the $\mu_\perp$ values measured at molecular surface areas of 10 and 6 nm^2 as a function of $DP_{PMLGSLG}$. It shows that at both molecular surface areas $\mu_\perp$ is highly dependent on the length of the PMLGSLG block. The decrease in $\mu_\perp$ upon monolayer compression from 10 to 6 nm^2/molecule may be attributed to the cancellation of the water dipole moments generated by the PMLGSLG block−water interaction as a result of the tilting of the block away from the water surface. At 6 nm^2/molecule, the increase in $\mu_\perp$ as a function of $DP_{PMLGSLG}$ arises from accumulation of the dipole moments of the PMLGSLG peptide units along the helix. For the $DP_{PMLGSLG}$ of 11 of CoPo_50_11, a part of the PMLGSLG block might be pulled into the water subphase to some extent because of its small length compared with the PLGA hydrophilic block. The dipole moments of the helix part in the subphase are screened by the water, resulting in a relatively low value of $\mu_\perp$ for CoPo_50_11 at 6 nm^2/molecule (Figure 6).

The entire molecule of the PLGA-*b*-PMLGSLG diblock copolymers in the double-brush monolayers at the air−water interface can be regarded as an α-helix with part of the helix immersed in the water subphase and the other part in the air

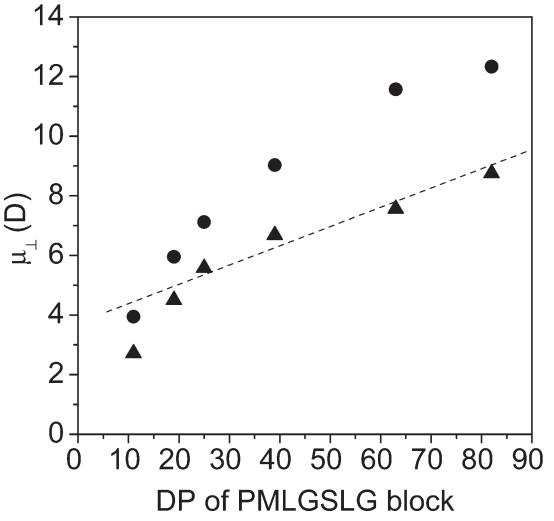

Figure 6. Effective molecular dipole moment ($\mu_\perp$) at molecular surface areas of 10 (circles) and 6 nm^2 (triangles) for the PLGA-*b*-PMLGSLG monolayers as a function of the $DP_{PMLGSLG}$.

medium. The dipole moment of the helix part in water is strongly suppressed. Nevertheless, for the part of the helix remaining in the hydrophobic layer, the increasing correlation between $\mu_\perp$ and the helix length indicates that the counteracting effects of the electrostatic reaction field generated by the water environment underneath is small. Though such a high-dielectric solvent as water may screen the charges distributed closely to the water surface, the effective dipoles of the polypeptide α-helices densely packed in air and tilted away from the water surface are significantly maintained.

In particular, the effect of reorientation of water molecules on monolayer spreading is significant, resulting in a large initial surface potential generated by the water. The cancellation of this initial surface potential due to the diminished interactions of the PMLGSLG hydrophobic block with the water surface upon tilting, along with the reorientation of the side chains toward the air and a change in local relative permittivities during molecular packing, can give rise to a decrease in the derived effective molecular dipole moment of the monolayer. As such, $\mu_\perp$ undergoes a larger change for the diblock copolymers of a larger $DP_{PMLGSLG}$ as shown in Figure 3.

Conclusions

For the first time, the surface potentials and effective molecular dipole moments for monolayers of α-helical amphiphilic diblock copolypeptides at the air−water interface were evaluated. Upon monolayer spreading, a large positive surface potential of hundreds of millivolts was produced by the interaction of the hydrophobic block of the diblock copolypeptides with the water surface. This behavior is strongly related to the surface area fraction of the block. The molecular dipole contributions, dependent on the conformation and the orientation of the polar groups, are not readily distinguished and can change significantly during the compression of the monolayer. In addition, due to the tilting of the PMLGSLG block to the surface normal, the cancellation of the dipole moments of water molecules generated upon monolayer spreading and probably a change in local relative permittivities during monolayer compression led to a gradual decrease in the derived effective molecular dipole moment of the monolayer. While the peptide dipoles of the α-helical hydrophilic block immersed in the subphase were effectively screened by the water, the screening effects on the peptide dipoles of the α-helical hydrophobic block appeared to be negligible. As a result, at the same average helix tilt angle, the monolayer molecular dipole moment effectively increased with increasing hydrophobic block length.

Acknowledgment. This research is supported by NanoNed, a nanotechnology program of the Dutch Ministry of Economic Affairs.